PHYSICS AND CHEMISTRY OF SOLID STATE
V. 25, No. 3 (2024) pp. 560-569
Section: Physics

DOI: 10.15330/pcss.25.3.560-569

Vasyl Stefanyk Precarpathian National University

ФІЗИКА І ХІМІЯ ТВЕРДОГО ТІЛА
Т. 25, № 3 (2024) С. 560-569
Фізико-математичні науки

PACS: 62.20.Qp; 71.15.Mb

ISSN 1729-4428 (Print)
ISSN 2309-8589 (Online)

S. Jerin Blessy[1], H. Johnson Jeyakumar[2], S. Gracelin Juliana[3], P. Selvarajan[4], A. Antony Muthu Prabhu[5]

Hardness, VSM, cyclic voltammetric and DFT studies of Cesium Sulphate-doped TGS crystals

[1] *Research scholar,Reg.No.21212152132003,PG and Research Department of Physics,Pope's College, Affiliated to Manonmaniam Sundranar University, Tirunelveli, Tamilnadu, India, jerinblessy1999@gmail.com;*
[2]*PG and Research Department of Physics, Pope's College, Affiliated to Manonmaniam Sundaranar University, Tirunelveli, Tamilnadu, India;*
[3]*Department of Physics, Nazareth Margoschis College, Nazareth, Tamilnadu, India;*
[4]*Department of Physics, Aditanar College of Arts and Science, Tiruchendur, Tamilnadu, India;*
[5]*Department of PG Chemistry, Aditanar College of Arts and Science, Tiruchendur, Tamilnadu, India*

The creation of capacitors, transducers, sensors, and infrared detectors utilise the nonlinear, ferroelectric triglycine sulphate (TGS) crystal. Cesium sulphate is incorporated into the lattice of TGS crystal to change its characteristics. Cesium sulfate-doped triglycine sulphate (CSTGS) single crystals were produced using a solution approach and a slow evaporation process. The title crystal was studied by single crystal XRD, FTIR, hardness, VSM, cyclic voltammetric and density functional theoretical (DFT) studies and the results are discussed in this paper.

Keywords: TGS; doping; solution growth technique, ferroelectric; FTIR; XRD; hardness; DFT; VSM; cyclic voltammetry.

Received 15 January 2024; Accepted 10 August 2024.

Introduction

Triglycine sulphate (TGS) crystal is a typical second-order ferroelectric phase transition at the Curie point T_c = 49 °C. TGS crystals have some disadvantages like fungal growth problems during the crystal growth compared to doped TGS crystals and to avoid the problems, many researchers added varieties of dopants into TGS crystals [1-5]. Despite the complex crystal and chemical structure, the ferroelectric phase transition in TGS follows the mean field behavior almost perfectly and the static dielectric properties can be quantitatively described by a simple Landau-Devonshire model. Newman et al. reported that crystals of triglycinesulfate are very interesting ferroelectric material and are widely used as room temperature IR detectors [6]. It is known that dopants can change the properties of the host crystals and therefore cesium sulfate was added as a dopant into the lattice of TGS crystals in this work. Ibrahim et al. have studied the effect of sulfuric acid doping on the growth and properties of TGS crystals [7] and they have also studied TGS crystals grown in acidic medium [8]. Manoharan et al. have synthesized calcium-doped triglycinesulfate single crystals [9]. Since unoded TGS crystal is easily depolarizable by applying voltage and voltage, many organic and inorganic dopants have been added into the lattice of TGS crystal by many authors to stabilize the internal domains [10-15]. Since no work on the addition of cesium sulfate to TGS crystals has been reported in the literature, we decided to grow a bulk single crystal of the title material using a solution method in combination with the slow evaporation technique and to characterize the grown crystals of cesium sulfate-doped triglycinesulfate (CSTGS) using different characterization studies like FTIR, VSM, Cyclic voltammetric and DFT studies.

I. Growth CSTGS crystals

Glycine of the Analar Reagent (AR) grade and concentrated sulfuric acid were combined in an aqueous solution at a 3:1 molar ratio. The solution was supplemented with 2 mol% cesium sulphate. For around three hours, the solution was continuously agitated with a magnetic stirrer before being filtered through four micro Whatman filter sheets. Then, a borosilicate glass beaker wrapped in porous paper was used to retain the filtrate. The growth vessel was stored in a quiet location. It was permitted to grow for roughly 25 to 30 days. The CSTGS sample's purity was raised through repeated crystallisation. Figure 1 is a typical example of a grown CSTGS crystal.

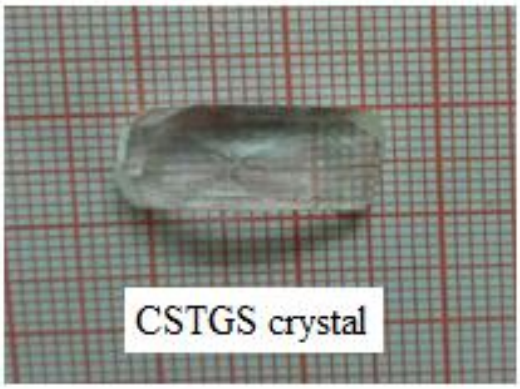

Fig.1. A grown crystal of CSTGS.

II. Results and discussion

2.1. FTIR studies.

The FTIR spectrum is a crucial tool for determining the various functional groups and chemical bonding interactions in a given substance. The Perkin-Elmer spectrometer was used to record it in the range 400 -4000 cm^{-1} and the obtained FTIR spectrum of the pellet of KBr-added CSTGS is shown in Fig. 2. The assignments to the absorption frequencies are given in accordance with the data reported in the literature [16]. The broad absorption band at 3109 corresponds to the NH_3^+ stretch mode. The CH stretching frequencies occur at 2601 and 2170 cm^{-1}. NH_3^+ bending and straining modes are likely due to absorption of IR frequencies at 1577, 1496, 685, and 501 cm^{-1}. Due to the CN Stretching mode, the absorption peak is at 1125 cm^{-1}. The IR absorption frequency at 926 cm^{-1} corresponds to SO_2 stretching. The FTIR assignments to all vibrational frequencies are given in Table 1.

2.2 Determination of mechanical parameters from microhardness measurement.

(i) Mircrohardness

The mechanical strength of a material plays an important role in device manufacture. Hardness is one of the mechanical parameters and is related to it the crystal structure of the material. In general, hardness is defi2ned as the ratio of applied load to area. Hardness depends on many parameters such as structure, thermal stability, composition, bond strength, etc. The hardness values can be used to calculate the elastic constants such as stiffness constant and yield point, and the elastic properties with thermal properties such as specific heat, coefficient of thermal expansion, Debye temperature and melting point [17, 18]. Hardness measurement can be divided into (i) microhardness measurement and (ii) macrohardness measurement. When low loads are applied to soft materials to measure hardness value, it is called micro hardness testing, and when high loads are applied to very hard materials like steel and metals to measure hardness, it is called macro hardness testing. The cut and polished CSTGS crystal is subjected to a static indentation Vickers microhardness study with a load ranging from 10 to 100 grams using a Shimadzu HMV-2 Vickers

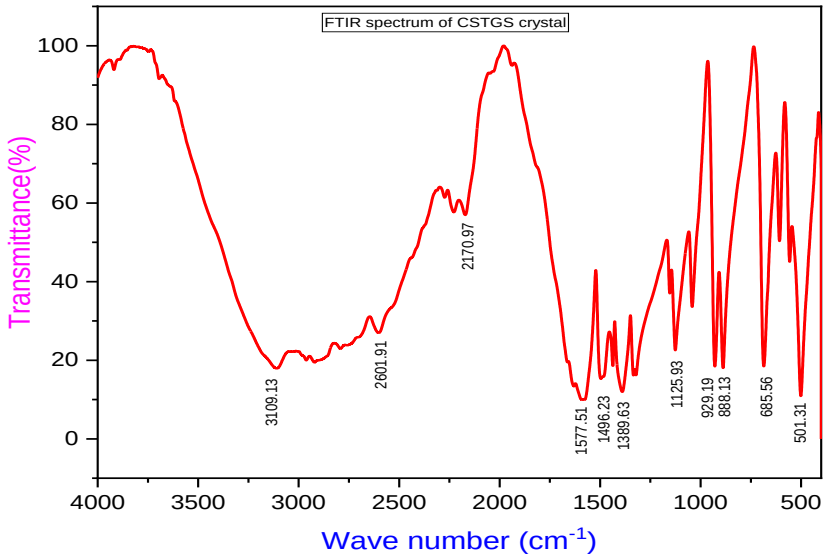

Fig. 2. FTIR spectrum of CSTGS crystal.

Table 1.
FTIR spectral assignments for CSTGS crystal

Wave number, (cm^{-1})	Assignments
3109	NH_3^+ stretching
2601	CH_2 stretching
2170	CH stretching
1577	NH_3^+ bending
1496	Coo^{-1} stretching
1389	CH_2 bending
1125	CN stretching
929	SO^{2-}stretching
888	C-C stretching
685	NH_3^+ torsion
501	NH_3^+ rocking

microhardness tester. The indentation time maintained for all applied loads is 10 seconds. For comparison purposes, the microhardness measurement was carried out both for undoped TGS and for cesium sulfate-doped TGS crystals. The average value of the diagonal indentation (d) was measured for each applied load and the variation of 'd' with load for undoped and CSTGS crystals is shown in Figure 4. Using the values of 'd' and the following relationship, the microhardness value of CSTGS crystal was determined.

$$H_v = 1.8544 \frac{P}{d^2} \qquad (1)$$

where P denotes the applied load and 1.8544 is a geometric factor constant for the pyramid shaped diamond indenter used to make an indentation on the surface of the sample. The variations in microhardness with applied stress for both undoped and CSTGS crystals are shown in Figure 4. The result shows that the hardness for both samples increases up to 70 g and then decreases slightly. It is found that microcracks form in the samples when the applied load is more than 100 g. The increase in hardness with loading is due to the reverse indentation size effect (RISE) [19]. It is observed that the hardness of the CSTGS crystal is higher than that of undoped TGS and this is due to the incorporation of cesium sulfate as ions in the interstitial positions of the host TGS crystal. For comparison, the hardness data in SI units for undoped TGS, CSTGS and diamond crystals are provided in Table 2 and it can be seen that diamond crystal is the hardest material as it has a hardness value of 92 GPa and title material is the less hard Crystal can only withstand low loads.

(ii) Work hardening coefficient

Eugene Meyer of the Materials Testing Laboratory of the Imperial School of Technology, Germany, developed Meyer's formula in 1908 as:

$$P = a_1 d_1^{n1} = a_2 d_2^{n2} = a_3 d_3^{n3} \qquad (2)$$

The above expression is applicable when many types of indenters are used. Since only one type of indenter was used in this work, the first term can be considered as:

$$P = a\, d^n \qquad (3)$$

where P is the stress, d is the average diagonal length of the indentation, a is constant and n is the strain hardening coefficient [20]. Using relationship (3), the work hardening coefficient (n) can be determined.

Equation (3) can be written as:

$$log_{10}(P) = log_{10}(a) + n log_{10}(d) \qquad (4)$$

and it is a straight line equation like y = mx + c,
where m is the slope and c is the y-intercept. A graph (Fig. 5) is drawn between log10(P) and log10(d) and the value of "n" is estimated to be 2.847 for undoped TGS crystal and obtained from Figure 6 to be 2.685 for CSTGS crystal.

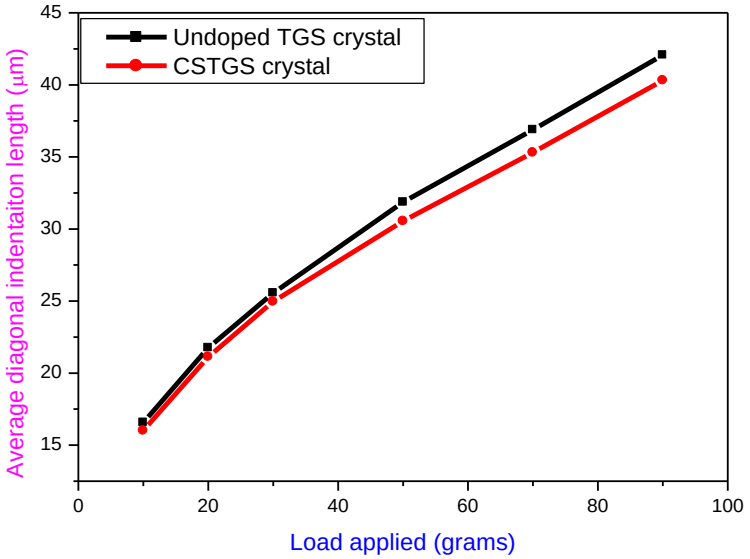

Fig. 3. Plot of average diagonal indentation versus applied load for CSTGS crystal.

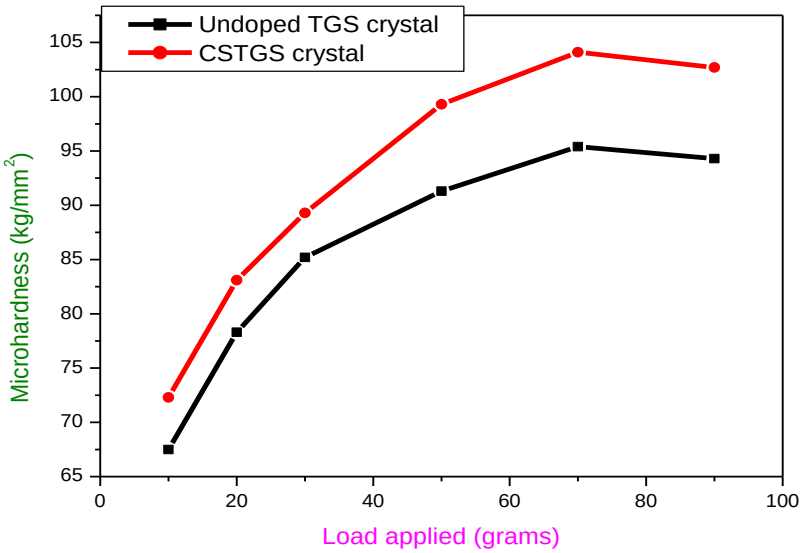

Fig. 4. Plots of microhardness versus applied load for undoped and cesium sulphate-doped TGS crystals.

Table 2.
Hardness data in SI units for undoped TGS, CSTGS and diamond crystals

Applied load	Vickers hardness (N/m^2 or pascal)		
	Undoped TGS x10^7	CSTGS crystal x10^7	Diamond crystal [30]
10 mN	66.15	70.85	-
20 mN	76.34	81.44	-
30 mN	83.46	87.51	-
50 mN	89.74	97.31	92 GPa at 5 N load
70 mN	93.42	102.02	
90 mN	92.42	100.65	

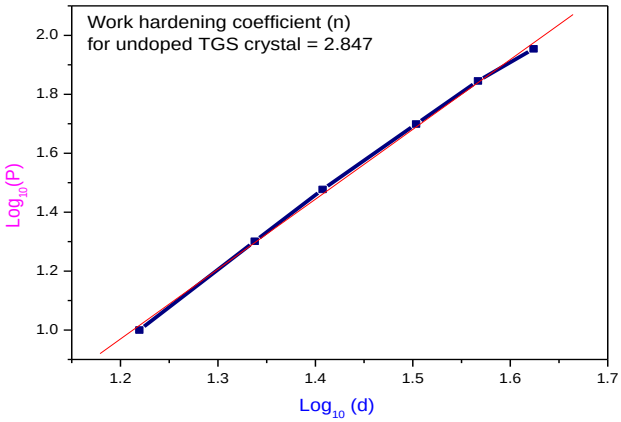

Fig. 5. Plot of $\log_{10}$(P) versus $\log_{10}$(d) for undoped TGS crystal.

The value of n is reported to be less than 1.6 for hard materials and greater than 1.6 for soft materials [21, 22] and therefore both undoped and cesium sulfate-doped TGS (CSTGS) crystals belong to Group of soft materials.

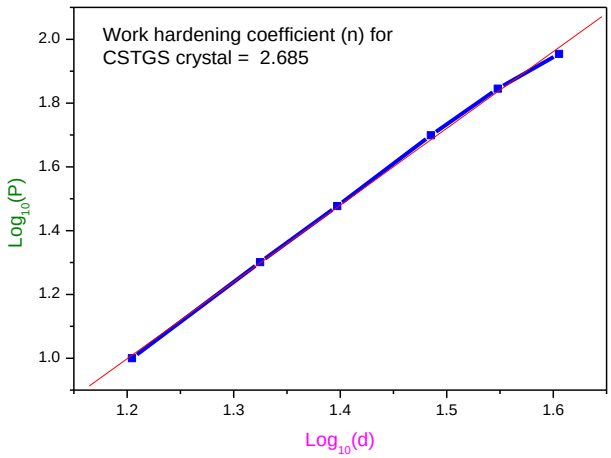

Fig. 6. Plot of $\log_{10}$(P) versus $\log_{10}$(d) for CSTGS crystal.

(iii) Stiffness constant

Elastic constants are used to explain the mechanical properties of solids. The elastic stiffness constant (C_{11}) is a measure of a material's ability to resist deformation and gives an indication of how atoms are bonded together to show the material's stiffness. This mechanical parameter can be calculated using the empirical formulaof Wooster [23] and is given by:

$$C_{11} = (H_v)^{7/4}, \qquad (5)$$

where H_v is the Vickers microhardness. The calculated elastic constant values of undoped and cesium sulfate-doped TGS crystals are shown in Figure 7. The elastic stiffness constant values are of the order of 10^{15} and hence the samples are very stiff to deformation. Since the stiffness constant is directly proportional to the hardness, it is observed that the variation of the stiffness constant with the applied load shows a behavior similar to that of the hardness.

(iv) Yield Strength

The yield strength is defined as the maximum stress that can be developed in a material without plastic deformation occurring and using the microhardness (H_v) and work hardening coefficient (n) values, the yield strength (Y) of the samples was calculated estimated and the relationship used for n > 2 is given below [24].

$$Y = (H_v/3)*(0.1)^{n-2} \quad (6)$$

Fracture toughness (K_c) is a measure of the relative level of resistance that the material offers without fracture and depends on factors such as crack size and applied load. It is calculated according to the following equation [25].

$$K_C = \frac{P}{\beta C^{3/2}}, \quad (7)$$

where C is the crack length from the indentation mark to the crack tip, P is the applied load and β = 7 is the geometric constant for the Vickers indenter.

The brittleness index (Bi) is an important mechanical property of the sample and a measure of fracture without deformation of the material and is determined with the following expression.

$$B_i = \frac{H_v}{K_c}. \quad (8)$$

Since the cracks are formed on the surface of the samples for the applied loads of 70 g and 90 g, the above mechanical parameters are calculated for these two loads and the values are given in Tables 3 and 4.

2.3 Second-order NLO studies.

The nonlinear optical (NLO) phenomena occur at sufficiently high intense laser fields. As the applied field strength increases, the polarization response of the medium is no longer linear and the induced polarization (P) becomes a non-linear function of the applied field and is given by

$$P = e_o c^{(1)} E + e_o c^{(2)} E^2 + e_o c^{(3)} E^3, \quad (9)$$

where ε_o is permittivity of free space or vacuum, E is the electric field and $\chi^{(1)}$, $\chi^{(2)}$ and $\chi^{(3)}$ are the first-order, second-order and third-order susceptibilities respectively. The second-order susceptibility, $\chi^{(2)}$ is responsible for second-order NLO phenomena like second harmonic generation (SHG), sum frequency generation (SFG),

Table 3.
Calculated mechanical parameters of undoped TGS crystal

Load	Yield strength x10^6 (N/m^2)	Fracture toughness (Nm$^{-3/2}$)	Brittleness Index x 10^6 (m$^{-1/2}$)
70 mN	70.235	602.141	1.694
90 mN	69.290	615.502	1.635

Table 4.
Calculated mechanical parameters of cesium sulphate-doped TGS crystal

Load	Yield strength x10^6 (N/m^2)	Fracture toughness (Nm$^{-3/2}$)	Brittleness Index x 10^6 (m$^{-1/2}$)
70 mN	64.365	596.408	1.566
90 mN	63.624	608.511	1.518

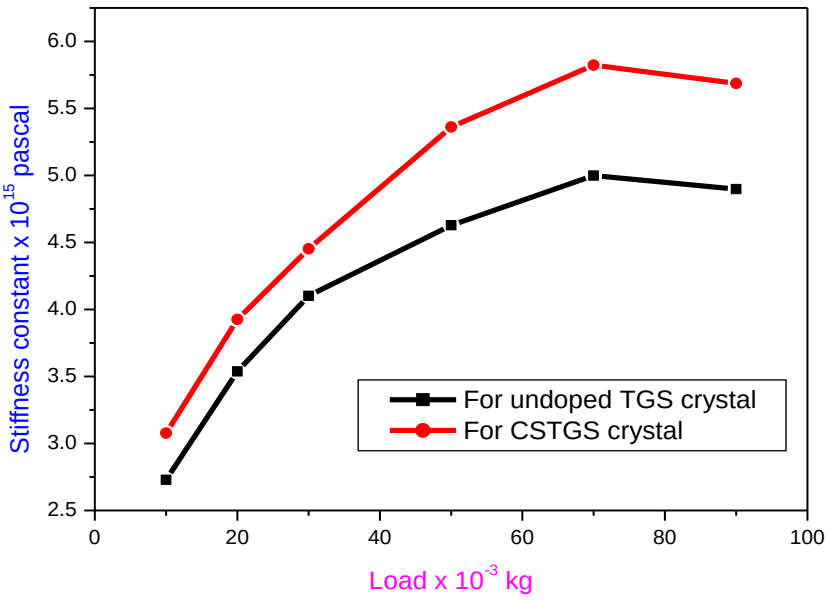

Fig. 7. Plots of stiffness constant versus applied load for undoped and cesium sulphate-doped TGS crystals.

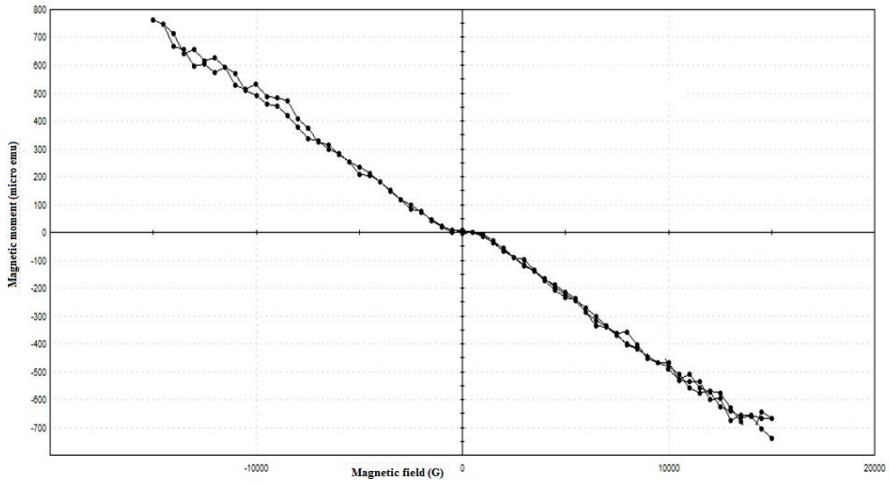

Fig. 8. The hysteresis loop for CSTGS crystal.

optical rectification etc. SHG efficiency was measured by the Kurtz-Perry technique [26] with 1064 nm radiation from a Q switched high-energy Nd:YAG laser with pulse width of 6 ns and repetition rate is 10 Hz. For this experiment, the grown crystal of CSTGS and the reference sample (KDP) were made into fine powder with the particle size of the order of 125 - 150 □m. When the sample was exposed to laser radiation of wavelength 1064 nm, green laser radiation of wavelength of 532 nm was emitted. Thus, the wavelength of incident radiation is reduced to half and hence the phenomenon is the SHG. For an input energy of laser radiation of 0.70 mJ/pulse, the SHG signal from CSTGS crystal was obtained to be 1.95 mJ/pulse and that from the reference sample KDP is 8.83 mJ/pulse. Thus, the relative SHG efficiency of CSTGS crystal is 0.22 times that of KDP. Compared to SHG efficiency of undoped TGS crystal (0.09 times that of KDP), CSTGS crystal has more SHG efficiency [27].

2.4. Crystal structure.

The crystal structure of cesium sulphate-doped TGS (CSTGS) crystal was found by using single crystal XRD method. ENRAF CAD-4 X-Ray diffractometer was used to find the unit cell parameters. The obtained values of lattice parameters are a = 9.214(3) Å, b = 12.975 (2) Å, c = 5.752(3) Å, □ = 90º, □□= 106.05(3)º, □□= 90º. Hence, CSTGS crystal belongs to the monoclinic structure.

2.5.VSM study.

At ambient temperature, the magnetic characteristics of the formed CSTGS crystal were investigated using a vibrating sample magnetometer (VSM) [28]. The hysteresis loop of magnetization of the material against the applied fields is shown in Figure 8. It displays the material's ferromagnetic characteristics as well as its responsiveness to an externally applied field. The ferromagnetic characteristics of material were determined using the hysteresis loop of a crystalline sample by applying a maximum field of 2000 G. The saturation magnetization and retentivityof CSTGS crystal are found ot be $752.19 \cdot 10^{-6}$ emu and $1.9960 \cdot 10^{-6}$ emu, respectively. The fields required to reduce magnetization to zero after saturation are known as coercivity, and its value is 40.131 G. Since CSTGS crystal has low coercivity, it belongs to soft ferromagnetic material.

2.6. Cyclic voltammetric study.

Cyclic voltammetric studies were carried out using a CHI 650c electrochemicalworkstation with conventional three electrode cell at room temperature. The reference electrode was a silver/silver chloride (Ag/AgCl) electrode, while the counter electrode was a platinum wire. Theelectrochemical properties of CSTGS crystal was investigated by means of cyclic voltammetry (CV) with potential window from 0 to to1.2 V at pH value of 7 (phosphate buffer solution) [29]. The recorded CV curves for the grown crystal with different scan rates such as 0.025 V/s, 0.05 V/s and 0.15 V/s are shown in the Figure 9. Strong redox behavior of the sample and asymmetric variationis observed during the scanning rate. It is discovered that the current rises when the scan rate is raised, pointing to the constructed CSTGS crystal's excellent capacitance behaviour.

2.7. Density functional theoretical (DFT) study.

Theoretical parameters, frontier molecular orbitals, Mulliken atomic charges, electrostatic potential map and natural bond orbital analysis were calculated for CSTGSS crystal. Various theoretical parameters of the sample from HOMO and LUMO energy values were determined using the relations given the literature [30-36]. The relevant software used to calculate the various parameters is NBO 6.0 software.

2.7.1. Structural parameters.

Table 5 gives the various structural parameters such as energy, EHOMO, ELUMO, energy gap, ionization potential, electron affinity, electronegativity, chemical potential, chemical hardness, chemical softness, dipole, electrophilicity index (□), electron accepting capability (□+), electron donating capability (□-), net electrophilicity (□□□), global softness (s), $\square E_{\text{Back donation}}$, nucleophilicity index (N), additional electronic charge($\square N_{max}$), optical softness (□0) were measured for

the investigated molecule using theoretical method.

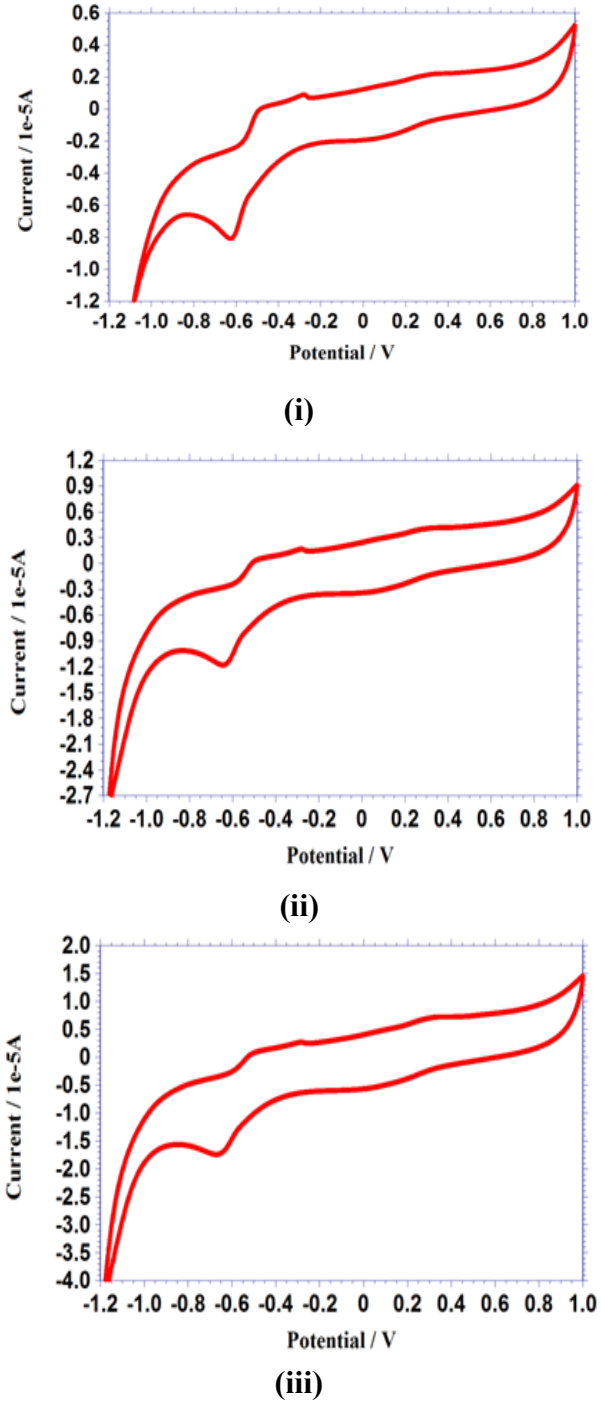

Fig. 9. Cyclic voltammetricbehavior of CSTGS crystal at (i) scan rate 0.025 V/s, (ii) scan rate 0.05 V/s and scan rate 0.1 V/s.

Electron affinity (A) and ionization potential (I) measure the ability of chemical species to accept and donate one electron. Using Koopman's theorem [37], the electron affinity and ionization potential can be replaced by the lowest unoccupied molecular orbital (LUMO) energy and highest occupied molecular orbital (HOMO) energy respectively. HUMO and LUMO behaviour of CSTGS crystal using density functional theory is shown in the Figure 10.

One of the most common chemical notions, electronegativity (χ) is the propensity of an atom or group to draw an electron towards itself. The energy difference between the occupied and unoccupied molecular orbitals is equivalent to global hardness (η). It is connected to another atomic characteristic called global softness (S). Electrophilicity is the capacity of an electrophile to accept electrons from a nucleophile.

Table 5.
Various parameters derived from the HOMO – LUMO values for the CSTGS crystal (DFT B3LYP 6-311G)

No.	Parameter	CSTGS
1	E_{HOMO}	-3.23
2	E_{LUMO}	-2.25
3	Energy gap (□E)	-0.97
4	Ionisation potential (I)	3.23
5	Electron affinity (A)	2.25
6	Electronegativity (□)	4.36
7	Chemical potential (□)	-4.36
8	Chemical hardness (□)	2.10
9	Chemical softness (S)	0.47
10	Electrophilicity index (ω)	4.51
10	Dipole	19.60
11	Energy (KJ/mol)	-970858.9287

Chemical potential and hardness have both been used in DFT to compute electrophilicity [38, 39].

The CSTGS sample's HOMO and LUMO have a -0.97 eV energy discrepancy. This molecule thus has the potential to be stable. The global hardness, softness, chemical potential, electronegativity, and electrophilicity indexof the sample are found to be 0.48; 2.05; -2.74; 2.74 and 7.72 eV respectively.

2.7.2. Molecular Electrostatic Potential Map.

Molecular electrostatic eventuality of a patch gives information about the parcels like molecular size, dipole moment, shape, electronic viscosity, hydrogen cling relations, and chemical reactivity etc. In molecular electrostatic eventuality, the shells are represented in red, blue, light blue, unheroic, and green colors. The red colour represents the electron-rich (incompletely negative charge) area whereas the blue colour represents the electron poor (incompletely positive charge) locales. Light blue colour represents slightly electron-deficient region while the unheroic colour represents a slightly electron-rich sphere. The green colour represents a neutral charge position. B3LYP/ 6 – 311 G system and the electrostatic implicit chart with different colour representation is shown in Figure 11. The region of red colour (electron-rich) is located around the oxygen tittles of one of the glycine patch in which electrophilic attack is possible. The green color region is located around the oxygen tittles of another two glycine motes. Blue colour region (electron-poor) region is spread each over the patch around hydrogen tittles which is prone to nucleophilic attack [40].

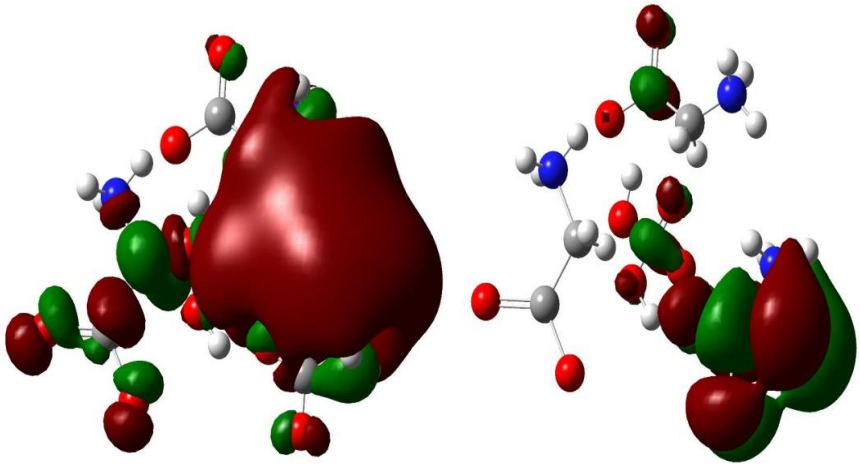

Fig. 10. HUMO and LUMO of CSTGS crystal using density functional theory.

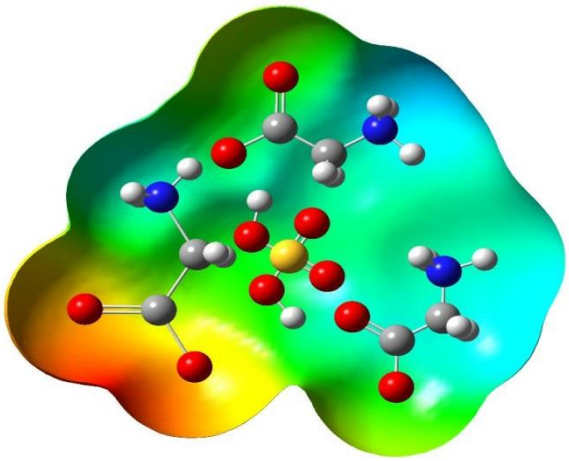

Fig. 11. Electrostatic potential map with different colours for CSTGS crystal.

Conclusions

2 mol% cesium sulfate was added to the aqueous solution prepared by incorporating glycine and sulfuric acid in a molar ratio of 3:1, and a slow evaporation method was adopted to grow the single crystals of cesium sulfate-doped triglycinesulfate (CSTGS). Single crystal XRD method reveals that CSTGS crystal crystallizes in monoclinic structure. The mechanical parameters such as hardness, work hardening coefficient, stiffness constant, yield strength, fracture toughness, brittleness index of the CSTGS crystal were estimated and analyzed. The functional groups of the sample were analyzed by the FTIR spectral method. The relative SHG efficiency of CSTGS crystal is obtained with 0.22 times that of t the KDP sample. Various structural parameters of the sample have been determined by DFT theory. Voltammetric study indicates that CSTGS crystal has good capacitance behaviour. Hysteresis loop of the title sample was obtained by VSM study and the result shows that the sample is a soft ferromagnetic material.

Acknowledgment

The authors are thankful to staff members of Cochin university (Cochin), St.Joseph's College (Trichy), Crescent Engineering college (Chennai), IIT (Madras), VOC college (Tuticorin), and VIT (Vellore) for having helped us to collect the research data and they thank the management and staff members of Pope's College, Sawyerpuram and Aditanar College of Arts and Science, Tiruchendur for the encouragement and support to carry out the research work.

S. Jerin Blessy – M.Sc, Research Scholar, Reg.No.21212152132003;
H. Johnson Jeyakumar – Ph.D, HOD and Associate Professor;
S. Gracelin Juliana – Ph.D, Associate Professor;
P. Selvarajan – Ph.D, HOD and Associate Professor;
A. Antony Muthu Prabhu – Ph.D , Assistant Professor.

[1] P. Selvarajan, B.N. Das, H.B. Gon, K.V. Rao, *Growth, Structural, Optical, Mechanical and Dielectric Characterization of Diammonium Hydrogen Phosphate (DAHP) Single Crystals.* J. Mater. Sci. 29, 4061 (1994); https://doi.org/10.4236/jmmce.2011.1015108.

[2] N. Balamurugan, M. Lenin, .G. Bhagavannarayana and P. Ramasamy, *Growth of TGS crystals using uniaxially solution-crystallization method of Sankaranarayanan-Ramasamy.* Crystal Res. Technol. 42, 151 (2007); https://doi.org/10.1002/crat.200610788.

[3] C. Berbecaru, H.V. Alexandru, L. Pintilie A, Dutu, B. Logofatu and Radulescu, *Doped versus pure TGS crystals*, Materials Sci. Engg. B. 11, 141 (2005); https://doi.org/10.1016/j.mseb.2004.12.069.

[4] Alexander McPherson, Alexander J. Malkin, Yu.G. Kuznetsov, Stanley Koszelak, *Investigations on Various Studies of TriglycineSulphophosphate Crystals Doped With Cesium Chloride.* J. Cryst. Growth 168, 74 (1996); https://doi.org/10.9790/4861-17002030914.

[5] R. Muralidharan, R. Mohankumar, P.M. Ushasree, R. Jayavel and P. Ramasamy, *Effect of rare- earth dopants on the growth and properties of triglycine sulphate crystals.* J.Crystal Growth. 234, 545 (2002); https://doi.org/10.1016/S0022-0248(01)01723-7.

[6] C.S. Fang, H. Liu, H.S. Zhuo, M. Wang and D. Xu, *A new modified TGS crystal.* Cryst. Res. Technol. 30, 785 (1993); https://doi.org/10.1002/crat.2170300612

[7] M.J. Ibrahim and T.M. Al-Saadi, IOP Conf. Ser.: Mater. Sci. Eng. 871, 012082 (2020); https://doi.org/10.1088/1757-899X/793/1/011001.

[8] Mher.J. Ibrahim and TagreedM.Al-Saadi, *Structural and Opticall Properties of Pure and doped Triglycine Sulphate Crystal Grown by slow evaporation technique",* AIPConfrence Proceedings 2123, 020015 (2019); http://dx.doi.org/10.1063/1.5116942.

[9] P. Manoharan and N. Neelakanda Pillai, Archives of Applied Science Research, 5(1), 93 (2013); http://scholarsresearchlibrary.com/archive.html.

[10] R.B. Lal & A.K. Batra, *Growth and properties of triglycine sulphate (TGS) crystals: Review*, Ferroelectrics, 142, 51 (1993);https://doi.org/10.1080/00150199308237884.

[11] X. Sun, M. Wang, Q.W. Pan, W. Shi, and C.S. Fang, *Study on the growth and properties of guanidine doped triglycine sulfate crystal*, Crystal Research and Technology, 34(10), 1251 (1999); https://ui.adsabs.harvard.edu/link_gateway/1999CryRT..34.1251S/doi:10.1002/(SICI)1521-4079(199912)34:10%3C1251::AID-CRAT1251%3E3.0.CO;2-G.

[12] K. Biedrzycki, *Energy distribution of electron emission from -α alanine doped TGS single crystals*, Solid State Communications, 118(3), 141 (2001); https://doi.org/10.1016/S0038-1098(01)00052-7.

[13] G. Su, Y. He, H. Yao, Z. Shi, and Q. Wu, *New pyroelectric crystal L-lysine-doped TGS (LLTGS)*, Journal of Crystal Growth, 209(1), 220 (2000); http://dx.doi.org/10.1016/S0022-0248(99)00591-6.

[14] S. Aravazhi, R. Jayavel, and C. Subramanian, *Growth and characterization of benzophenone and urea doped triglycine sulphate crystals*, Ferroelectrics, 200(1-4), 279 (1997); https://doi.org/10.1080/00150199708008612.

[15] N.T. Shanthi, P. Selvarajan, and C.K. Mahadevan, *Studies on TriglycineSulfate (TGS) crystals doped with sodium bromide NaBr grown by solution method*, Indian Journal of Science and Technology, 3, 49 (2009); https://doi.org/10.17485/ijst/2009/v2i3/29414.

[16] V.V. Ghazaryan, M. Fleck, A.M. Petrosyan, Spectrochimica Acta Part A 78, 128, (2011); https://doi.org/10.1016/j.saa.2010.09.009.

[17] J.M. De Man, F.W.Wood ,*Hardness of Butter.I. Influence of Season and Manufacturing Method Microindentation hardness testing*, J. Dairy Sci.41, 360 (1958); https://doi.org/10.3168/jds.S0022-0302(58)90928-7.

[18] Y.L. Ke, F.X. Dong, *Hardness of materials: studies at levels from atoms to crystals*. Chinese Sci. Bull. 54, 131 (2009); https://doi.org/10.1007/s11434-008-0550-8.

[19] P.N. Kotru, Sushma Bhat and K.K. Raina, *Microhardness measurements on single crystals of gel-grown rare-earth (Nd) molybdate and paramolybdate*, J. Mater., Sci. Lett. 8, 587, (1989); https://doi.org/10.1007/BF00720308.

[20] E. Meyer, Z. ver. Deut. Ing. 52, 645, (1908);

[21] S. Balamurugan, P.Ramasamy, *Bulk growth of <101> KDP crystal by Sankaranarayanan – Ramasamy method and it's characterization*, Mater. Chem. Phy. 112, 1, (2008); https://doi.org/10.1016/j.matchemphys.2008.05.058.

[22] P.J. Blau, B.R.Lawn, Microindentation Techniques in Materials Science and Engineering, (1985).

[23] W.A. Wooster, *Physical properties and atomic arrangements in crystals*, Rep. Progr. Phys. 16, 62, (1953); https://doi.org/10.1088/0034-4885/16/1/302.

[24] M. N. Ravishankar, M. A. Ahlam, R. Chandramani and A. P. Gnana Prakash, *"Comparative Study of Mechanical, Dielectric and Electrical Properties of Solution Grown Semi-Organic NLO Crystal Glycine with Additives-Ammonium Oxalate, Potassium and Barium Nitrate",* Indian Journal of Pure and Applied Physics, 51, 55-59 (2013).

[25] B.R Lawn, E.R Fuller, *Equilibrium penny-like cracks in indentation fracture*. J. Mater. Sci. 10, 2016 (1975); http://dx.doi.org/10.1007/BF00557479.

[26] K Nihara, R Morena, D.P.H. HHasselman, *Evaluationof KIc of brittle solids by the indentation method with low crack-to-indent ratios.* J. Mater. Sci. Lett. 1, 13, (1982); https://doi.org/10.1007/BF00724706.

[27] S.S. Kurtz and T. Perry, *A powder technique for the evaluation of nonlinear optical materials.* J. Appl. Phys. 39, 3798, (1968); http://dx.doi.org/10.1063/1.1656857.

[28] M. Krishna Mohan, S. Ponnusamy, C. Muthamizhchelvan, Optics and Laser Technology 97, 321 (2017); https://doi.org/10.1142/s0219581x17600365.

[29] K. Thilaga, P. Selvarajan, S.M. Abdul Kadar, Photoluminescence, Impedance, *Thermal Characteristics and Hirshfeld Surface Analysis of Potassium Bisulphate Single Crystals for Third Order NLO Applications.East European Journal of Physics*, 145, (2021); https://doi.org/10.26565/2312-4334-2021-4-19.

[30] L. Bányai, Y.Z. Hu, M. Lindberg, S.W. Koch, Phys. Rev. B Condens. Matter Mater. Phys, 38, 8142 (1988); https://doi.org/10.1007/978-1-4615-3726-7_41.
[31] N. SurendraBabu, D. Jayaprakash, *Global and reactivity descriptors studies of cyanuric acid tautomers in different solvents by using of density functional theory (DFT).* Int J Sci Res 4:,615 (2015); https://www.ijsr.net/getabstract.php?paperid=19051501.
[32] H. Ouafy, M. Aamor, M. Oubenali, M. Mbarki, EL.A. Haimouti, EL T. *Ouafy Molecular Structure, electrostatic potential and HOMO, LUMO studies of 4-aminoaniline, 4-nitroaniline and 4-isopropylaniline by* DFT. Sci Tech Asia 27, 9 (2002); https://ph02.tci-thaijo.org/index.php/SciTechAsia/article/view/242269.
[33] L.W. Chung, W.M.C. Sameera, R. Ramozzi, A.J. Page, M. Hatanaka, G.P. Petrova, K. Morokuma, *The ONIOM method and its applications*. Chem Rev 115, 5678 (2015); https://doi.org/10.1021/cr5004419.
[34] E.D. Glendening, C.R. Landis, F. Weinhold, NBO 6.0: *Natural bond orbital analysis program*. J Comp Chem 34, 1429 (2013); https://doi.org/10.1002/jcc.23266.
[35] L.I.U. Shu-Bin, *Conceptual density functional theory and some recent developments*, Acta Phys. Chim. Sin. 25(3), 590 (2009); https://doi.org/10.3866/PKU.WHXB20090332.
[36] P. Geerlings, F. De Proft, W. Langenaeker, *Conceptual density functional theory*, Chem. Rev. 103(5), 1793 (2003); https://doi.org/10.1021/cr990029p.
H. Chermette, *Chemical reactivity indexes in density functional theory*, J. Comput.Chem. 20(1), 129 (1999); https://doi.org/10.1002/(SICI)1096-987X(19990115)20:1%3C129::AID-JCC13%3E3.0.CO;2-A.
[37] L.H. Mendoza-Huizar, *Chemical reactivity of isoproturon, diuron, linuron, and chlorotoluron herbicides in aqueous phase: a theoretical quantum study employingglobal and local reactivity descriptors*, J. Chem. 1, 9 (2015); https://doi.org/10.1155/2015/751527.
[38] P.K. Chattaraj, U. Sarkar, D.R. Roy, *Electrophilicity index*, Chem. Rev. 106(6), 206 (2006); https://dpi.org/10.1021/cr040109f.
[39] Z. Demircioglu, A. Kastas, O. Buyukgungor, *Theoretical analysis (NBO, NPA, Mulliken Population Method) and molecular orbital studies (hardness, chemical potential, electrophilicity and Fukui function analysis) of €-2-((4-hydroxy-2-methylphenylimino)methyl)-3-methoxyphenol*, J. Mol. Struct. 1091, 183 (2015); https://doi.org/10.1016/j.molstruc.2015.02.076.

С. Дж. Блессі[1], Х. Дж. Джеякумар[2], С. Г. Джуліана[3], П. Селвараджан[4], А.Е.М. Прабху[5]

Твердість, вібраційна магнітометрія, циклічна вольтамперометрія та DFT-дослідження кристалів Тригліцин Сульфату, легованих Сульфатом Цезію

[1]*Факультет фізичних досліджень, Папський коледж при університеті Манонманіам Сундаранар, Тірунелвелі, Таміл Наду, Індія, jerinblessy1999@gmail.com;*
[2]*PG та відділ дослідницької фізики, Папський коледж при університеті Манонманіам Сундаранар, Тірунелвелі, Тамілнаду, Індія;*
[3]*Фізичний факультет, коледж Назарет Маргошіс, Назарет, Тамілнаду, Індія;*
[4]*Фізичний факультет, коледж мистецтв і науки Адітанар, Тіручендур, Тамілнаду, Індія;*
[5]*Кафедра PG хімії, Адітанарський коледж мистецтв і науки, Тіручендур, Тамілнаду, Індія*

Нелінійний сегнетоелектричний кристал тригліцинсульфату (TGS) часто використовують для створення конденсаторів, перетворювачів, датчиків та інфрачервоних детекторів. Для зміни його характеристик у кристалічну решітку вводять Сульфат цезію (TGS). Монокристали тригліцинсульфату, легованого сульфатом цезію (CSTGS), отримували з розчину та повільного процесу випаровування. Кінцевий кристал досліджували методами XRD, FTIR, вивченням твердості, VSM, циклічною вольтамперометрією та теоретичними дослідженнями методом функціоналу густини (DFT). Отримані результати обговорюються в цій статті.

Ключові слова: тригліцину сульфат; легування; техніка вирощування з розчину, сегнетоелектрик; FTIR; XRD; твердість; DFT; VSM; циклічна вольтамперометрія.